Mathematical Modelling of MHD Casson Nanofluid Blood Flow with Thermal Radiation in a Dilated Stenosed Artery

Abstract

To investigate the numerical simulation of nanoparticle-enhanced non-Newtonian blood flow with internal heat generation in a dilated stenotic artery using the Casson fluid framework and analyze the effects of various parameters on flow characteristics.

The governing mathematical model is formulated applying the Casson fluid framework and transformed into a system of ordinary differential equations, which is solved numerically using the bvp4c solver in Maple. Graphical and tabular illustrations are used to examine key flow characteristics including velocity and temperature profiles, local Nusselt number and skin-friction coefficient.

The results show that velocity increases with rising curvature flow parameter, stenosis height, and nanoparticle volume fraction, whereas it drops with increasing magnetic field parameter and Casson fluid parameter. Temperature increases with Casson fluid parameter, curvature parameter, stenosis height, and magnetic field strength, but decreases with nanoparticle volume fraction, Prandtl number, and thermal radiation parameter. A slight but noticeable variation is observed between alumina (Al_2O_3) and ferric oxide (Fe_3O_4) nanoparticles with respect to the volume-fraction parameter.

The study provides valuable insights into the behavior of nanofluid blood flow in stenosed arteries, which may guide the development of effective therapeutic and diagnostic techniques for cardiovascular diseases. The numerical approach using bvp4c solver proves effective for analyzing complex hemodynamic phenomena.

Keywords: Casson Nanofluid; Thermal Radiation; Dilated Artery; Alumina; Cardiovascular; Magnetohydrodynamic

2020 Mathematics Subject Classification: 76Z05; 76W05; 80A20; 92C35

1 Introduction

Nanoparticles are ultrafine materials, typically ranging from 1–100 nm in size, and are invisible to the naked eye without advanced electron microscopy. Their interaction with blood flow has attracted substantial attention due to their potential applications in targeted delivery of drugs, biomedical diagnostics, and the analysis of blood rheology. When introduced into the bloodstream, nanoparticles can significantly influence hemodynamic characteristics and thermal behavior, particularly in diseased vessels.

Ahmed and Nadeem (2016) demonstrated that incorporating nanoparticles such as copper, titanium dioxide, and aluminum oxide can alter the hemodynamic properties of blood flowing through stenosed arteries while exhibiting antimicrobial effects that may aid prevent infections in diseased vessels. Similarly, Sarwar et al. (2022) investigated thermal enhancement in blood nanofluid flow through stenotic arteries using gold nanoparticles within a Sisko non-Newtonian fluid model. Their investigations indicated improved thermal performance and highlighted the potential of nanoparticles for localized drug delivery in regions of restricted blood flow.

Stenosis, defined as the constriction of an artery, is primarily caused by atherosclerotic plaque formation, inflammation, or hereditary disorders. It represents a significant cardiovascular risk factor due to its ability to restrict blood flow and increase the likelihood of severe complications such as ischemic stroke and myocardial infarction. Understanding the interaction between nanoparticles and stenosed arteries is therefore essential for advancing therapeutic and diagnostic strategies. In this context, alumina (Al_2O_3) and ferric oxide (Fe_3O_4) nanoparticles have gained particular attention due to their thermal, magnetic, and biocompatible properties, which can strongly influence flow behavior and arterial wall interactions.

Several recent works highlight the growing interest in employing nanoparticles for biomedical applications. Jerka et al. (2024) examined nanoparticle-mediated influences on endothelial cell transport, while Zuberi et al. (2024) investigated thermophoresis and Brownian motion in Casson nanofluid flows over nonlinear stretching surfaces. Their results provide deeper insights into nanoparticle-driven transport phenomena relevant to heat transfer and biomedical engineering.

Past studies have also explored the advantages of various nanoparticle materials. Shahzad et al. (2022), Karmakar et al. (2023), and Muthtamilselvan et al. (2023) focused on gold nanoparticles owing to their unique optical properties and imaging capabilities. Conversely, Gandhi et al. (2023) and Das et al. (2023) investigated alumina and iron oxide nanoparticles for their magnetic responsiveness, enabling targeted delivery within stenotic regions. Titanium dioxide nanoparticles have also been used due to their biocompatibility and photocatalytic activity, offering therapeutic potential in vascular medicine.

Copper and alumina nanoparticles have shown distinct benefits in modulating physiological processes such as oxidative stress, inflammation, and endothelial dysfunction—key contributors to stenosis progression (Haris et al., 2024; Lin et al., 2024). Their tunable physicochemical properties permit precise targeting of arterial walls, enabling localized therapy while minimizing systemic side effects. However, challenges such as nanoparticle aggregation, altered effective viscosity, and deviations from Newtonian fluid behavior must also be considered.

The use of hybrid nanoparticles has expanded rapidly. Studies by Poonam et al. (2022), Khanduri et al. (2024), Jalili et al. (2023), and Manchi & Ponalagusamy (2022) examined the synergistic effects of combining different nanoparticle types—such as gold-silver or silica-iron oxide hybrids—to enhance imaging, cooling efficiency, or drug delivery capabilities in stenosed arteries. Other researchers have explored magneto-bio-hybrid nanofluids (Basha et al., 2022), thrombosis generation using magnetic fields (Hussain et al., 2023), and tri-hybrid nanofluids in Casson fluid models (Karmakar et al., 2023). These works collectively underscore the growing applicability of nanoparticle-enhanced fluids in treat-

ing vascular diseases.

More recent investigations include the effects of magnetic fields on heat transfer (Kabeel et al., 2015), magnetohydrodynamic hybrid nanofluid flow for drug delivery (Alghamdi et al., 2021), electromagnetic hybrid nano-blood pumping (Das et al., 2021), and sophisticated computational approaches such as machine-learning-assisted predictions of blood flow parameters in stenosed arteries (Li et al., 2024). Studies by Zuberi et al. (2024) and Dhange et al. (2025) further expanded the understanding of nanofluid behavior under complex arterial geometries and force-field interactions.

Motivated by these developments, the present study focuses on a Casson nanofluid model with water as the base fluid and alumina (Al_2O_3) and ferric oxide (Fe_3O_4) nanoparticles. The aim is to address critical gaps in existing research by examining the combined effects of nanoparticles, thermal radiation, magnetic field, and arterial dilation on blood flow and heat transfer in stenotic arteries. This work provides new insights that may guide the development of effective therapeutic and diagnostic techniques for cardiovascular diseases.

2 Formulation of the Problem

The geometry of this present problem can be expressed mathematically as Bhuvana et al. (2016):

$$R(x) = \begin{cases} R_0 - \frac{\delta}{2}\left[1 + \cos\frac{2\pi}{l_i}\left(\bar{x} - \beta_i - \frac{l_i}{2}\right)\right], & \beta_i \leq \bar{x} \leq \omega_i, i = 1, 2 \\ R_0, & \text{otherwise} \end{cases} \tag{1}$$

where $R(x)$ represents the radius of the artery in the stenosed part, R_0 represents the radius of the artery in the absence of stenosis, l_i is the irregular section length, $\wp$ is a constant, δ is critical height, which develops in two different locations $\bar{x} = \beta_1 + \frac{l_0}{2}$ and $\bar{x} = \beta_2 + \frac{l_0}{2}$.

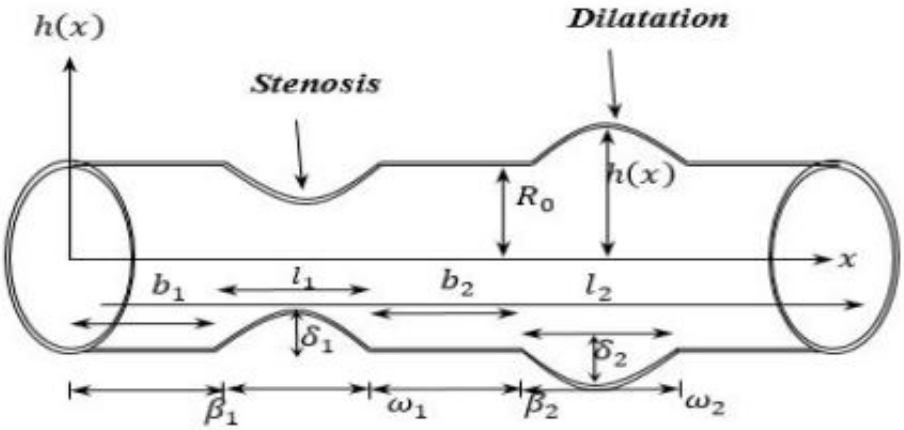

Figure 1. Geometry of the fluid flow

The blood flow is modelled in arteries by Navier-Stokes equations for blood flow through a cylindrical artery Das et al. (2021) are:

$$\frac{\partial(ru)}{\partial x} + \frac{\partial(rv)}{\partial r} = 0, \tag{2}$$

$$\rho_{\mathrm{nf}}\left(u\frac{\partial}{\partial x} + v\frac{\partial}{\partial r}\right)u = \mu_{\mathrm{nf}}\left(1+\frac{1}{\beta}\right)\left(\frac{\partial^2 u}{\partial r^2} + \frac{1}{r}\frac{\partial u}{\partial r}\right) - \sigma B(x)^2, \tag{3}$$

$$(\rho C_p)_{\mathrm{nf}}\left(u\frac{\partial}{\partial x} + v\frac{\partial}{\partial r}\right)T = k_{\mathrm{nf}}\left(\frac{\partial^2 T}{\partial r^2} + \frac{1}{\bar{r}}\frac{\partial T}{\partial r}\right) - \frac{\partial q_r}{\partial r} \tag{4}$$

The equation for the radiative flux (q_r) is defined as a result of Rosseland's approximation as:

$$\frac{\partial q_r}{\partial r} = -\frac{4\sigma^*}{3k^*}\frac{\partial T^4}{\partial r} \tag{5}$$

where R, $\mu_{\rm nf}$, $\rho_{\rm nf}$, $k_{\rm nf}$, B, σ, C_p and T are the radius of the artery, dynamic blood viscosity, the blood density, Intensity of magnetization, electric conductivity of the blood, thermal conductivity, specific heat capacity and blood temperature in radial direction respectively. $\beta = \frac{\mu_b\sqrt{2\pi_k}}{\tau_y}$ represents the material parameter of Casson fluid, μ_b is the plastic dynamic viscosity, τ_y the yield stress of the flow, $2\pi_k$ is the critical value of the product based on the non-Newtonian model.

The corresponding boundary conditions for the modelling equations are:

$$u = 0, \quad v = 0, \quad T = T_0, \quad \text{at } r = R(x) \tag{6}$$

$$\frac{\partial u}{\partial r} = 0, \quad \frac{\partial T}{\partial r} = 0, \quad \text{at } r = 0 \tag{7}$$

The thermal attributes of nanofluids as described by Haris et al., 2024 are employed in this research and are given by:

$$\frac{\rho_{\rm nf}}{\rho_f} = \left((1-\phi) + \phi\frac{\rho_s}{\rho_f}\right), \tag{8}$$

$$\frac{\mu_{\rm nf}}{\mu_f} = \frac{1}{(1-\phi)^{\frac{5}{2}}}, \tag{9}$$

$$\frac{(\rho C_p)_{\rm nf}}{(\rho C_p)_f} = \left((1-\phi) + \phi\frac{(\rho C_p)_{\rm nf}}{(\rho C_p)_f}\right), \tag{10}$$

$$\frac{k_{\rm nf}}{k_f} = \frac{k_s + 2k_{bf} - 2\phi(k_{bf} - k_s)}{k_s + 2k_{bf} + 2\phi(k_{bf} - k_s)}. \tag{11}$$

The equation of continuity embedded in Equation (2) is satisfied trivially by considering:

$$u = \frac{1}{r}\frac{\partial \psi}{\partial r}, \quad v = -\frac{1}{r}\frac{\partial \psi}{\partial x}, \tag{12}$$

where ψ is the stream function.

Using Equation (8) and taking into account the subsequent dimensionless parameters:

$$u = \frac{u_0 x}{L_0} F'(\eta), \quad v = -\frac{R}{r}\sqrt{\frac{u_0 v_f}{L_0}} F(\eta), \tag{13}$$

$$\eta = \frac{r^2 - R^2}{2R}\sqrt{\frac{u_0}{v_f L_0}}, \quad \theta(\eta) = \frac{T - T_0}{T_1 - T_0}, \tag{14}$$

$$\psi = \sqrt{\frac{u_0 x^2 v_f}{L_0}} R F(\eta). \tag{15}$$

The equations presented in (3) and (4) transform to:

$$\frac{\left(1 + \frac{1}{\beta}\right)}{T_1 T_2}\left[(1 + 2\xi\eta)F''' + 2\xi F''\right] + \left(FF'' - F'^2 - MF'\right) = 0 \tag{16}$$

$$\frac{1}{T_3 T_4 \mathrm{Pr}}\left[(1 + 2\xi\eta)\theta'' + 2\mathrm{Rd}\xi\theta'\right] + \left(F\theta' - \theta F'\right) = 0 \tag{17}$$

where

$$T_1 = (1-\phi)^{\frac{5}{2}}, \tag{18}$$

$$T_2 = (1-\phi) + \phi\frac{\rho_s}{\rho_f}, \tag{19}$$

$$T_3 = \left((1-\phi) + \phi\frac{(\rho C_p)_{\mathrm{nf}}}{(\rho C_p)_f}\right), \tag{20}$$

$$T_4 = \frac{k_s + 2k_{bf} + 2\phi(k_{bf} - k_s)}{k_s + 2k_{bf} - 2\phi(k_{bf} - k_s)}. \tag{21}$$

Considering the dimensionless parameters outlined in Equation (10), the particular boundary conditions specified in Equation (5) are altered to:

$$F(0) = 0, \quad F'(0) = 0, \quad \theta(0) = 1 \quad \text{at } \eta = 0, \tag{22}$$

$$F''(\eta) = 0, \quad \theta'(\eta) = 0 \quad \text{at } \eta = 0 \tag{23}$$

The following dimensionless variables are introduced:

$$\mathrm{Pr} = \frac{k_f}{(\mu C_p)_f}, \quad \mathrm{Rd} = \frac{4\sigma^* T_\infty^3}{k^* k}, \tag{24}$$

$$M = \frac{\sigma B^2}{(C_p)_{\mathrm{nf}}}, \quad \xi = \sqrt{\frac{L_0 v_f}{u_0 R^2}}. \tag{25}$$

where Pr denotes Prandtl's number, M the magnetic parameter, Rd represents thermal radiation parameter and ξ curvature flow parameter.

The important parameters, namely the heat transfer coefficient (Nusselt number, Nu) and the skin friction coefficient C_f, characterizing the flow field, are elucidated as follows:

$$C_f = \frac{\tau_w}{\frac{1}{2}\rho_f U_w^2}, \quad \mathrm{Nu} = \frac{x q_w}{k_f(T_w - T_\infty)}. \tag{26}$$

Now, the drag force τ_w and thermal flux q_w are given by:

$$\tau_w = \mu_{\mathrm{nf}} \left.\frac{\partial u}{\partial r}\right|_{r=R}, \quad q_w = -k_{\mathrm{nf}} \left.\frac{\partial T}{\partial r}\right|_{r=R} \tag{27}$$

By integrating dimensionless parameters as outlined in Equation (9), Equation (14) assumes the following structure:

$$C_f = \frac{1}{T_1 \mathrm{Re}_x^{\frac{1}{2}}} F''(0), \quad \mathrm{Nu}_x = -\frac{k_{\mathrm{nf}}}{k_f} \mathrm{Rd}\, \theta'(0). \tag{28}$$

$\mathrm{Re}_x^{\frac{1}{2}}$ in Equation (17) refers to local Reynold's number.

Table 1: Thermo-physical properties of base fluid and nanoparticle

Property	**Base fluid (Blood)**	**Alumina (Al_2O_3)**	**Ferric Oxide (Fe_3O_4)**
ρ (kg/m^3)	1063	3970	4000
k (W/mK)	0.492	40	2
C_p (J/kgK)	3594	765	700
ξ (K^{-1})	18000	85000	–

3 Method of Solution

The complexity of the modeled problem necessitated the utilization of an advanced numerical technique, the bvp4c module in Maple since while dealing with intricate boundary value problems that involve non-linearities, stiff equations, or complex

boundary conditions, conventional solvers struggle to produce accurate results efficiently. In such cases, the bvp4c solver shines by offering robust solutions with high accuracy and stability. Its versatility allows it to handle various problems across various domains, providing researchers and engineers with a powerful tool to model and analyze complex phenomena effectively. The importance of the bvp4c module lies in its ability to overcome the challenges posed by complex boundary value problems, enabling users to gain valuable insights and make informed decisions in fields ranging from engineering and physics to biology and finance. In the current problem, the non-linear coupled ordinary differential equations (Eqs.(10) and (11)), along with their boundary conditions (Eq.(13)), are solved numerically using the shooting technique implemented with the bvp4c solver, the built-in function in the computational tool Maple. At this stage, the higher-order system of equations is converted into a first-order system as follows:

$$F = p_1, \quad F' = p_1' = p_2, \quad F'' = p_2' = p_3, \tag{29}$$

$$F''' = p_3', \quad \theta = p_4, \quad \theta' = p_4' = p_5, \quad \theta'' = p_5' \tag{30}$$

where

$$F''' = \frac{-2\xi F'' - T_1 T_2 \left(FF'' - F'^2 - MF'\right)}{(1 + 2\xi\eta)} \tag{31}$$

$$\theta'' = \frac{-2\mathrm{Rd}\xi\theta' - T_3 T_4 \mathrm{Pr}\left(F\theta' - F'\theta\right)}{(1 + 2\xi\eta)} \tag{32}$$

Initial guesses are required for the bvp4c solver, which iteratively refines the solution by adjusting step sizes until the desired precision is achieved. The choice of initial guess

and boundary layer thickness depends on the parameter values used. A tolerance of 0.000001 for this problem is considered. A suitable numerical code is developed for this purpose, and the results obtained are presented in graph form.

4 Results and Discussion

The numerical simulation of Alumina and Ferric oxide nanoparticles on non-Newtonian blood flow through a stenotic and post stenotic artery with heat transfer via bvp4c module in Maple has been considered in this present study. To facilitate analysis, the governing differential equations are initially normalized and then solved using the 4th order collocation method, bvp4c module in Maple. Through this methodology, the study reveals velocity and temperature profiles, shedding light on the significance of relevant parameters within the biomedical context. To carry out the numerical solution, various thermo-physical properties of blood, alumina and ferric oxide nanoparticles embedded in Table 1 are utilized. The numerical values of various physical parameters are taken in the ranges: $0.001 \leq \phi \leq 0.2$; $0.1 \leq \gamma \leq 0.4$; $0.1 \leq M \leq 2.2$; $3.6 \leq \mathrm{Pr} \leq 6$; $0.1 \leq \mathrm{Rd} \leq 1.2$. The chosen numerical values not only reflect the physiological characteristics of blood and the materials infused but also account for the complex interplay of forces involved, including the influence of magnetic field and thermal radiation. Through this meticulous calibration, the simulations can provide insights into the dynamic behavior of blood flow in stenosed artery, offering valuable information for biomedical research and potential treatment strategies. Thus, the selected numerical values represent a realistic portrayal of fluid dynamics in stenosed arteries, facilitating a deeper understanding of this critical physiological phenomenon.

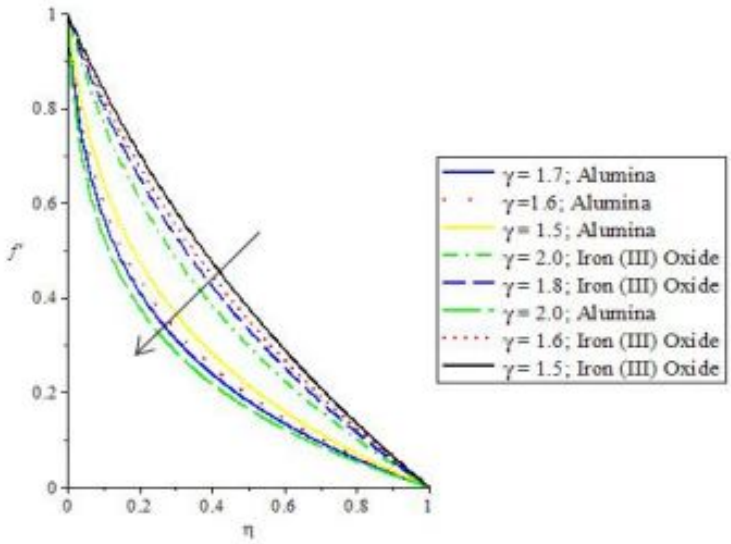

Figure 2: Velocity profiles for distinct values of Curvature flow parameter

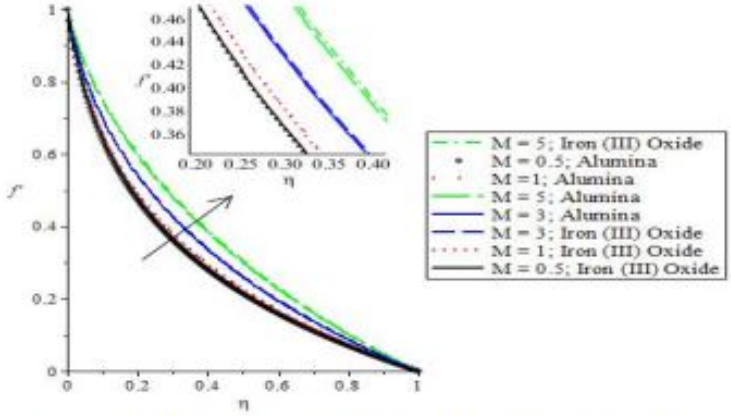

Figure 3: Velocity profiles for distinct values of magnetic parameter

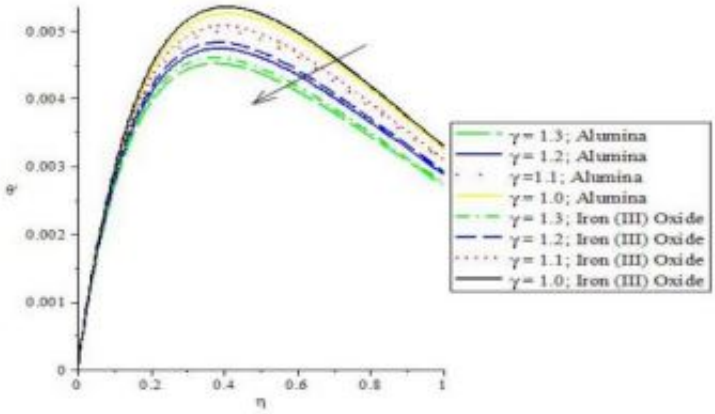

Figure 4: Temperature profiles for distinct values of Curvature flow parameter

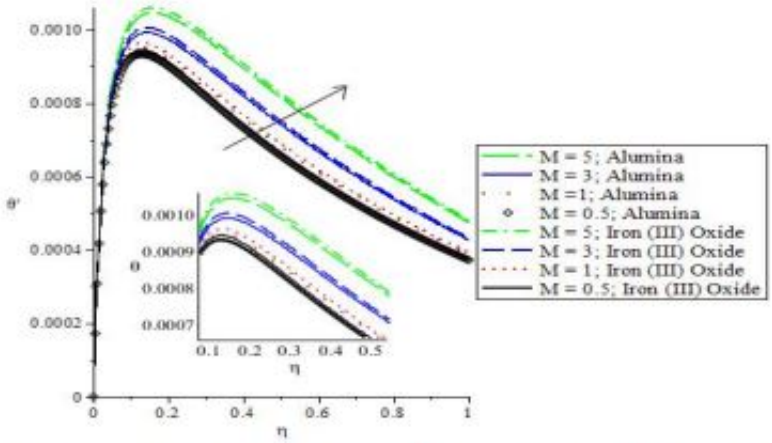

Figure 5: Temperature profiles for distinct values of Magnetic parameter

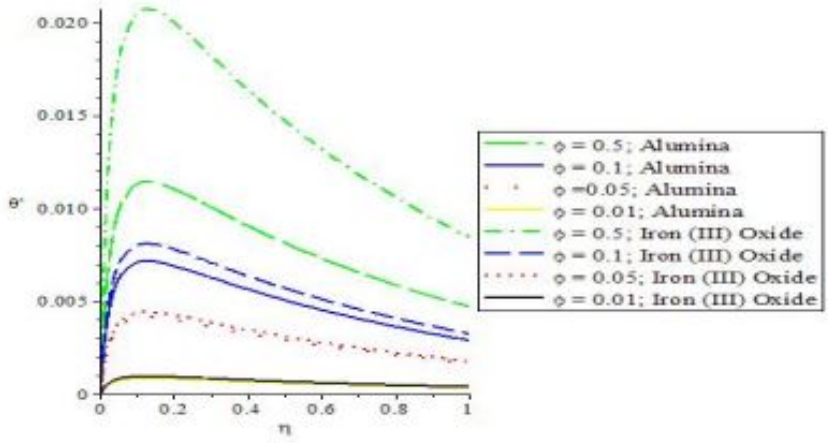

Figure 6: Temperature profiles for distinct values of Curvature flow parameter

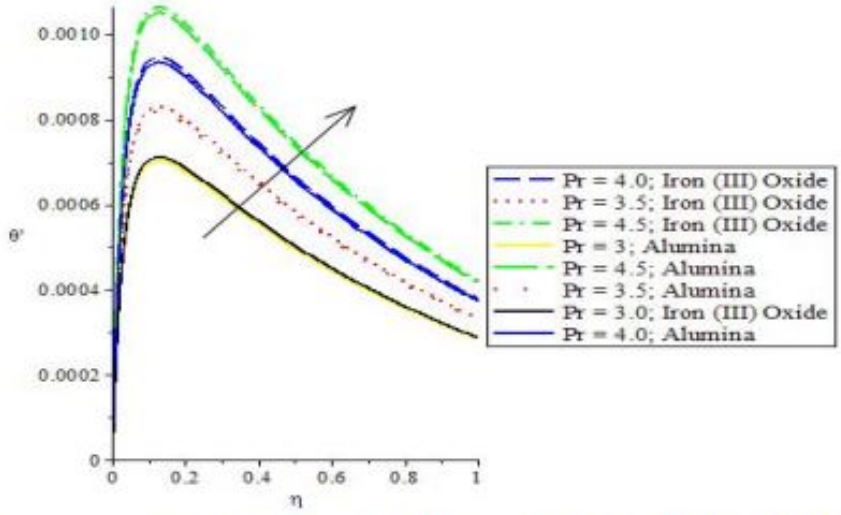

Figure 7: Temperature profiles for distinct values of Prandtl number

figure 8- Temperature profiles for distinct values of thermal radiation

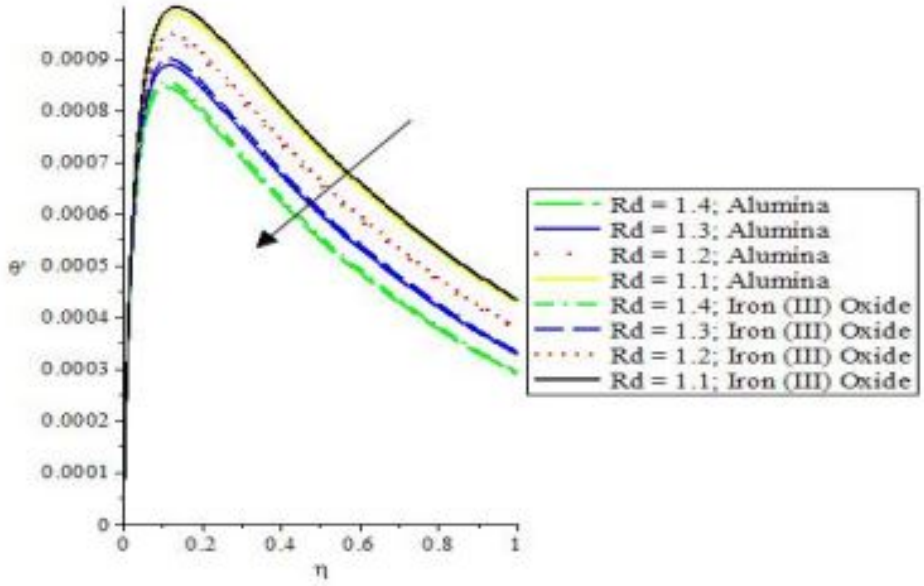

Table 2: Comparison of Nusselt Number for Al_2O_3 Nanoparticles with Haris et al. (2024) for Rd = 1

ϕ	**Present Study**	**Haris et al. (2024)**	**% Error**
0.10	2.43352	2.43366	0.0057%
0.13	2.39458	2.39367	0.0380%
0.16	2.34755	2.34680	0.0320%
0.10	2.43361	2.43377	0.0066%
0.13	2.76032	2.75763	0.0976%
0.16	3.01784	3.01882	0.0324%

Table 3: Comparison of Skin-Friction Coefficient for Al_2O_3 Nanoparticles with Haris et al. (2024) for Rd = 1

ϕ	**Present Study**	**Haris et al. (2024)**	**% Error**
0.10	3.02572	3.02311	0.0862%
0.13	3.00458	3.00865	0.1351%
0.16	3.00117	3.00126	0.0030%
0.10	3.02458	3.02700	0.0800%
0.13	2.68034	2.68012	0.0081%
0.16	2.35378	2.34269	0.4734%

5 Conclusion

The present study investigated the numerical simulation of Alumina and Ferric Oxide nanoparticles in a non-Newtonian Casson blood flow with internal heat generation through a dilated stenotic artery. Based on the obtained results, the following conclusions are drawn:

- **Temperature behaviour:** The temperature profile increases with rising Casson fluid parameter, curvature parameter, stenosis height, and magnetic field strength. Conversely, temperature decreases with increases in nanoparticle volume fraction, Prandtl number, and thermal radiation parameter.
- **Velocity behaviour (increase):** The velocity profile increases with higher curvature parameter, stenosis height, and nanoparticle volume fraction.
- **Velocity behaviour (decrease):** The velocity profile decreases as the magnetic field parameter and the Casson fluid parameter increase.
- **Nanoparticle comparison:** Alumina nanoparticles show a stronger response to changes in the volume fraction parameter compared to Ferric Oxide. However, both nanoparticles exhibit no significant differences in other parameter variations.

Nomenclature

$R(x)$	Radius of the artery in the stenosed region
R_0	Radius of the artery in the healthy (non-stenosed) region
l_i	Length of the irregular stenosed section
$\wp$	Constant (dimensionless parameter)
δ	Critical height of the stenosis
q_r	Radiative heat flux
R	General notation for artery radius
μ_{nf}	Dynamic viscosity of nanofluid (blood-based)
ρ_{nf}	Density of nanofluid (blood-based)
k_{nf}	Thermal conductivity of nanofluid
B	Magnetic field strength
σ	Electrical conductivity of blood
C_p	Specific heat capacity at constant pressure
T	Blood temperature in the radial direction
$\beta = \mu_b/2\pi_k$	Casson fluid parameter (non-Newtonian model)
μ_b	Plastic dynamic viscosity of Casson fluid
τ_y	Yield stress of Casson fluid
$2\pi_k$	Critical value based on the non-Newtonian model

References

1. A. Ahmed and S. Nadeem, *The study of (Cu, TiO_2, Al_2O_3) nanoparticles as anti-microbials of blood flow through diseased arteries*, J. Mol. Liq. **216** 615–623, 2016.

2. R. Manchi and R. Ponalagusamy, *Modeling of pulsatile EMHD flow of Au-blood in an inclined porous tapered atherosclerotic vessel under periodic body acceleration*, Arch. Appl. Mech. **91** (7) 3421–3447, 2021.

3. L. Sarwar, A. Hussain, U. Fernandez-Gamiz, S. Akbar, A. Rehman and E. S. M.

Sherif, *Thermal enhancement and numerical solution of blood nanofluid flow through stenotic artery*, Sci. Rep. **12** (1) 17419, 2022.

4. D. Jerka, K. Bonowicz, K. Piekarska, S. Golyer, U. S. Derici and O. A. Hindy, *Unraveling endothelial cell migration: insights into fundamental forces, inflammation, biomaterial applications, and tissue regeneration strategies*, ACS Appl. Bio Mater. **7** (4) 2054–2069, 2024.

5. H. A. Zuberi, M. Lal, S. Verma and N. A. Zainal, *Computational investigation of brownian motion and thermophoresis effect on blood-based Casson nanofluid on a non-linearly stretching sheet*, J. Adv. Res. Numer. Heat Transfer **18** (1) 49–67, 2024.

6. S. M. Mousavi, A. A. R. Darzi, O. Ali Akbari, D. Toghraie and A. Marzban, *Numerical study of biomagnetic fluid flow in a duct with a constriction affected by a magnetic field*, J. Magn. Magn. Mater. **473** 42–50, 2019.

7. D. F. Jamil, R. Roslan, M. Abdulhamed, N. Che-Him, S. Sufahani and M. Mohamad, *Unsteady blood flow with nanoparticles through stenosed arteries in the presence of periodic body acceleration*, J. Phys.: Conf. Ser. **995** 012032, 2018.

8. B. Vasu, A. Dubey, O. A. Beg and R. S. R. Gorla, *Micropolar pulsatile blood flow conveying nanoparticles in a stenotic tapered artery: non-Newtonian pharmacodynamic simulation*, Comput. Biol. Med. **126** 104025, 2020.

9. P. Karmakar and S. Das, *Electro-blood circulation fusing gold and alumina nanoparticles in a diverging fatty artery*, BioNanoScience **13** (2) 541–563, 2023.

10. F. Shahzad, W. Jamshed, F. Aslam, R. Bashir, E. S. M. TagElDin and H. A. E. W. Khalifa, *MHD pulsatile flow of blood-based silver and gold nanoparticles between two concentric cylinders*, Symmetry **14** (11) 2254, 2022.

11. M. Muhtamilselvan and Y. Gifteena Hingis, *Flow characteristics of gold nanoparticles and microorganisms in a multistenotic artery treated with a catheter*, Aust. J. Mech. Eng. 1–16, 2023.

12. R. Gandhi, B. Sharma, Q. M. Al-Mdallal and H. Mittal, *Entropy generation and shape effects analysis of hybrid nanoparticles (Cu-Al_2O_3/blood) mediated blood flow through a time-variant multistenotic artery*, Int. J. Thermofluids **18** 100336, 2023.

13. S. Das, P. Karmakar and A. Ali, *Simulation for bloodstream conveying bi-nanoparticles in an endoscopic canal with blood clot under intense electromagnetic force*, Wave Random Complex 1–38, 2023.

14. B. K. Sharma, U. Khanduri, N. K. Mishra, I. Albajjan and L. M. Perez, *Entropy generation optimization for the electroosmotic MHD fluid flow over the curved stenosis artery in the presence of thrombosis*, Sci. Rep. **13** (1) 15441, 2023.

15. Y. Lin, R. Lin, H. B. Lin and S. Shen, *Nanomedicine-based drug delivery strategies for the treatment of atherosclerosis*, Med. Drug Discov. **22** 100189, 2024.

16. Poonam and B. K. Sharma, *Mathematical analysis of hybrid nanoparticles (Au-Al_2O_3) on MHD blood flow through a curved artery with stenosis and aneurysm using hematocrit-dependent viscosity*, In: Nonlinear Dynamics and Applications, Cham: Springer, 407–419, 2022.

17. U. Khanduri and B. Sharma, *Mathematical analysis of hall effect and hematocrit dependent viscosity on Au/GO blood hybrid nanofluid flow through a stenosed catheterized artery with thrombosis*, In: International Workshop of Mathematical Modelling, Applied Analysis and Computation, Springer **17** 121–137, 2024.

18. P. Jalili, A. Sadeghi Ghahare, B. Jalili and D. Domiri Ganji, *Analytical and numerical investigation of thermal distribution for hybrid nanofluid through an oblique artery with mild stenosis*, SN Appl. Sci. **5** (4) 95, 2023.

19. R. Manchi and R. Ponalagusamy, *Pulsatile flow of EMHD micropolar hybrid nanofluid in a porous bifurcated artery with an overlapping stenosis in the presence of body acceleration and joule heating*, Braz. J. Phys. **52** (2) 52, 2022.

20. H. T. Basha, K. Rajagopal, N. A. Ahammad, S. Sathish and S. R. Gunakala, *Finite difference computation of Au Cu/magneto-bio-hybrid nanofluid flow in an inclined uneven stenosis artery*, Complexity **2022** 1–18, 2022.

21. A. Hussain, M. N. R. Dar, W. K. Cheema, Y. Han and R. Kanwal, *Clinical symbiosis of hybrid nanoparticles and induced magnetic field on heat and mass transfer in multiple stenosed artery with erratic thrombosis*, Sci. Rep. **13** (1) 15588, 2023.

22. P. Karmakar and S. Das, *Modeling non-Newtonian magnetized blood circulation with tri-nanoadditives in a charged artery*, J. Comput. Sci. **70** 102031, 2023.

23. S. Das, B. Barman, R. Jana and O. Makinde, *Hall and ion slip currents impact on electromagnetic blood flow conveying hybrid nanoparticles through an endoscope with persistaltic waves*, BioNanoScience **11** (3) 770–792, 2021.

24. M. Arif, L. Di Persio, P. Kumam, W. Watthavu and A. Akgul, *Heat transfer analysis of fractional model of couple stress Casson tri-hybrid nanofluid using dissimilar shape nanoparticles in blood with biomedical applications*, Sci. Rep. **13** (1) 4596, 2023.

25. T. Nazar and M. Shabbir, *Irreversibility analysis in the ternary nanofluid flow through an inclined artery via Caputo-Fabrizio fractional derivatives*, Results Phys. **53** 106992, 2023.

26. A. Kabeel, E. M. El-Said and S. Dafea, *A review of magnetic field effects on flow and heat transfer in liquids: present status and future potential for studies and applications*, Renew. Sustain. Energy Rev. **45** 830–837, 2015.

27. W. Alghamdi, A. Alsubie, P. Kumam, A. Saeed and T. Gul, *MHD hybrid nanofluid flow comprising the medication through a blood artery*, Sci. Rep. **11** (1) 11621, 2021.

28. Y. Li, D. Wan, D. Hu and C. Li, *A novel approach for estimating blood flow dynamics factors of eccentric stenotic arteries based on ML*, Eng. Anal. Bound. Elem. **163** 175–185, 2024.

29. P. G. Geredeli, H. Kunwar and H. Lee, *Partitioning method for the finite element approximation of a 3D fluid-2D plate interaction system*, Numer. Methods Partial Differ. Equ. **40** (6) e23132, 2024.

30. H. A. Zuberi, M. Lal, S. Deo, A. Saxena, O. A. Beg, S. Kuharat et al., *Computational hemodynamics of Sisko blood doped with gold and silver nanoparticles in a stenosed artery with porous walls*, Numer. Heat Transf. A: Appl. (in press), 2024.

31. H. A. Zuberi, M. Lal, A. Singh, N. A. Zainal and A. J. Chamkha, *Numerical simulation of blood flow dynamics in a stenosed artery enhanced by copper and alumina nanoparticles*, Comp. Model. Eng. Sci. 2024.

32. R. V. Bhuvana, K. P. Maruthi and C. Umadevi, *A mathematical model for micropolar fluid flow through an artery with the effect of stenosis and post stenotic dilatation*, Appl. Appl. Math. **11** 680–692, 2016.